Istraživanja i projektovanja za privredu
ISSN 1451-4117
DOI:10.5937/jaes0-69390
www.engineeringscience.rs

iipp publishing

Journal of Applied Engineering Science
Original Scientific Paper,
Volume 24, Number 4, Year 2026,
no 1370, pp 781-795

LEAKAGE-SUPPRESSED ROTATING-HOUSING ARCHIMEDES SCREW TURBINE FOR LOW-HEAD MICRO-HYDROPOWER: EXPERIMENTAL PERFORMANCE AND PREDICTIVE OPTIMIZATION

Rahmad Hidayat*, Heri Wibowo, Fredy Surahmanto

Universitas Negeri Yogyakarta, Faculty of Engineering, Department of Mechanical Engineering, Yogyakarta, Indonesia

**rahmadhidayat.2023@student.uny.ac.id*

Leakage through the radial clearance between screw blades and stationary housing contributes to hydraulic losses in conventional Archimedes screw turbines (ASTs). This study evaluates a leakage-suppressed rotating-housing AST (RH-AST) through experimental investigation, computational fluid dynamics (CFD), and regression-based operating-condition optimization for low-head micro-hydropower applications. The proposed configuration integrates the screw blades and cylindrical housing into a single rotating assembly, structurally eliminating the conventional radial leakage pathway. Laboratory experiments were conducted at flow rates of 50–100 L/min, inclination angles of 20°–30°, and a controlled rotational speed of 45 RPM. CFD simulations employing the Volume of Fluid (VOF) method and SST k–ω turbulence model were used to examine hydraulic behavior and assess torque predictions. Second-order polynomial regression models were developed to estimate torque, mechanical power, and hydraulic efficiency. The RH-AST achieved maximum experimental values of 0.99 Nm, 4.65 W, and 46.71%, respectively, at 100 L/min and 30°. Compared with the fixed-housing configuration, mean torque increased by up to 89.07%. CFD exhibited a mean absolute relative torque deviation of 23.56%, while the regression models achieved in-sample R^2 values of 0.9956, 0.9959, and 0.9892, respectively. Constrained optimization identified a maximum predicted efficiency of 46.56% at 100 L/min and 30°. These findings establish a preliminary model-assisted framework for identifying favorable RH-AST operating conditions within the investigated domain, although independent predictive validation remains necessary.

Keywords: Archimedes screw turbine, rotating-housing configuration, gap leakage suppression, computational fluid dynamics, response surface optimization, constrained optimization, micro-hydropower

HIGHLIGHTS

- A rotating-housing Archimedes screw turbine structurally removes the conventional radial leakage pathway.
- Laboratory experiments achieved 0.99 Nm torque and 4.65 W mechanical power at 100 L/min and 30°.
- CFD captured qualitative hydraulic trends, with a 23.56% mean absolute relative torque deviation.
- Regression-based optimization identified favorable operating conditions within the tested domain.

1 Introduction

Increasing demand for sustainable and decentralized energy systems has led to greater interest in renewable technologies that can be implemented in rural and low-resource regions [1]. Among various renewable energy technologies, micro-hydropower systems are recognized for their stable power generation, long operational life, and relatively low environmental impact, making them particularly suitable for decentralized renewable energy deployment and rural electrification in remote areas with limited grid accessibility [1–6]. In low-head applications, the Archimedes Screw Turbine (AST) has attracted considerable attention due to its simple construction, reported fish-friendly operation, debris tolerance, and capability to operate efficiently at hydraulic heads below 5 m [5, 7–11]. AST systems are also recognized for their relatively low ecological impact, owing to their slow rotational speed, reduced disturbance to sediment transport processes, and improved compatibility with aquatic ecosystems compared with conventional low-head hydropower technologies.

Previous studies have shown that AST performance is strongly influenced by geometric and operating parameters such as blade pitch, inclination angle, filling level, rotational speed, and discharge conditions [12–14]. Fundamental analytical relationships governing screw geometry and volumetric behavior were established by Rorres [12] which subsequently supported the development of experimental investigations, leakage modeling, CFD simulations, and predictive optimization approaches for AST systems [5, 15–19]. Recent CFD studies further revealed that internal flow characteristics, pressure distribution, vortex formation, recirculation zones, and free-surface interactions significantly affect hydraulic efficiency and energy conversion mechanisms in AST systems [20,21]. Advanced multiphase modeling approaches based on the Volume of Fluid (VOF) method have enabled more accurate representation of air–water interfaces and internal hydrodynamic behavior under varying operating conditions [20–22].

Despite these developments, the efficiency of conventional fixed-housing AST systems remains limited by leakage flow through the radial clearance between rotating blade tips and stationary housing surfaces. This leakage creates bypass flow that reduces water occupancy inside the screw buckets and weakens the hydrostatic loading responsible for torque generation. Recent studies have identified gap leakage, overflow leakage, and outlet power losses as significant mechanisms contributing to hydraulic energy dissipation and reduced turbine efficiency [10, 17, 23–25]. Previous experimental and CFD investigations demonstrated that leakage flow also promotes vortex formation, recirculation zones, and hydraulic energy dissipation within the screw channels [22, 26]. Although previous studies attempted to reduce leakage losses through geometric optimization and leakage prediction models [25, 27], most existing approaches still treat leakage as an unavoidable hydraulic phenomenon that must be modeled or mitigated rather than structurally eliminated.

From a power engineering perspective, leakage losses become increasingly critical in low-head micro-hydropower systems because the available hydraulic energy is inherently limited [2, 4]. Therefore, directly eliminating dominant leakage pathways offers significant potential for improving energy conversion efficiency. Previous studies briefly evaluated rotary or closed-trough screw turbine concepts [28]; To the best of the authors' knowledge, comprehensive investigations focusing on leakage elimination mechanisms, internal hydrodynamic behavior, and predictive optimization of rotating-housing AST systems remain very limited. In contrast to conventional fixed-housing designs, this study proposes a leakage-suppressed rotating-housing Archimedes Screw Turbine in which the screw blades and housing are integrated into a single rotating assembly, thereby eliminating the radial clearance responsible for gap leakage.

The main contributions of this study are threefold: (i) development of a leakage-suppressed rotating-housing AST concept that structurally eliminates radial gap leakage, (ii) experimental and CFD-based investigation of its hydraulic performance under varying operating conditions, and (iii) development and validation of regression-based predictive models for performance optimization.

In addition to experimental investigation, this study also addresses the limited availability of predictive optimization models specifically developed for leakage-suppressed AST systems. Existing predictive approaches are primarily based on conventional fixed-housing configurations and may not accurately represent the altered hydraulic behavior introduced by leakage elimination [15, 17, 25, 27, 29]. Accordingly, this study combines experimental investigation, CFD analysis, and predictive optimization to evaluate the performance of the rotating-housing AST under low-head operating conditions and to establish quantitative relationships between operating parameters and turbine performance characteristics, extending previous efforts that typically considered only CFD or parametric optimization in conventional fixed-housing systems [15, 22, 26, 27].

The analysis focuses on torque generation, mechanical power output, hydraulic efficiency, internal flow behavior, and predictive performance relationships under varying operating conditions. The findings are expected to support the development of more efficient and scalable low-head micro-hydropower systems for decentralized renewable energy applications.

2 Materials and methods

2.1 Turbine design

Two laboratory-scale Archimedes Screw Turbine (AST) prototypes were developed to compare the hydraulic and mechanical performance between conventional fixed-housing and leakage-suppressed rotating-housing configurations, as shown in Figure 1. The geometric design of both turbines generally followed the low-head AST configuration reported in previous experimental studies on screw turbine performance and hydraulic optimization [12, 16, 29]. The primary geometric parameters included screw length, outer diameter, shaft diameter, pitch ratio, blade number, and inclination angle.

In the conventional fixed-housing configuration, the screw rotated independently inside a stationary cylindrical housing, with a radial clearance of 2 mm between the blade tips and the inner housing surface. This clearance prevented mechanical contact during rotation but also provided a potential bypass-flow pathway between adjacent screw chambers [27, 30]. In contrast, the rotating-housing configuration mechanically integrated the screw blades and cylindrical housing into a single rotating assembly, thereby structurally removing the conventional blade–housing radial clearance. The principal screw geometry was maintained identical between the two configurations to enable a controlled performance comparison. Accordingly, the observed differences in turbine performance were evaluated relative to the fixed-housing prototype incorporating a 2-mm radial clearance.

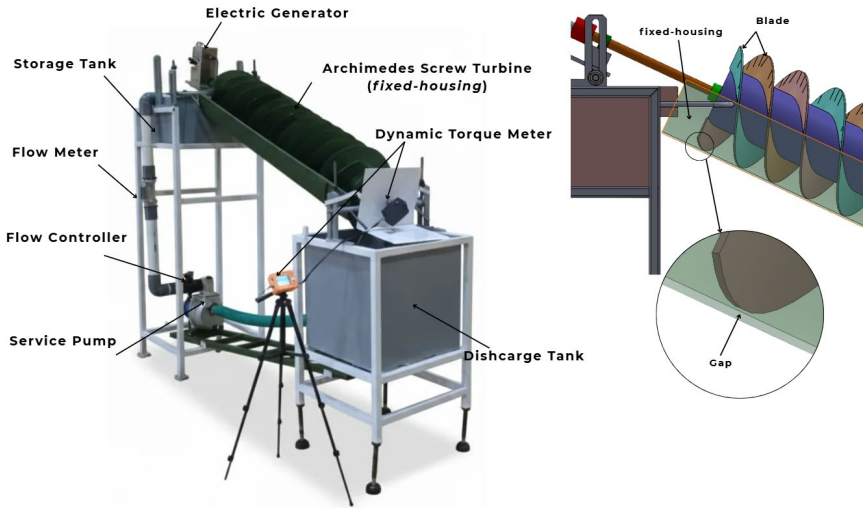

(a)

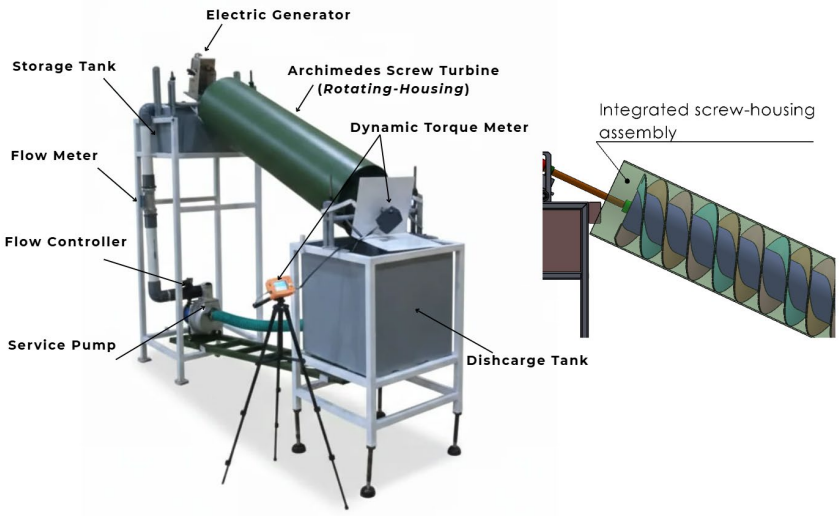

(b)

Fig. 1. Experimental AST prototypes: (a) fixed-housing configuration; (b) rotating-housing configuration

The turbine components were fabricated using laboratory-scale manufacturing methods to ensure dimensional consistency between both configurations. Several inclination angles and discharge conditions were investigated to evaluate the influence of operating parameters on torque generation, mechanical power output, and hydraulic efficiency. The geometric specifications of the turbine prototypes are summarized in Table 1.

Table 1. Geometric parameters of the experimental ast prototypes

Parameter	Symbol	Value	Unit
Outer diameter	D	0.316	m
Shaft diameter	d	0.168	m
Blade pitch	P	0.318	m
Turbine axial length	L	1.200	m
Effective installation length for head calculation	L_{eff}	1.221	m
Number of blade	N	3	-
Inclination angle	θ	20, 25, 30	deg
Housing type	-	Fixed / Rotating	-
Radial clearance, fixed-housing	c	0.002	m
Blade–housing clearance, rotating-housing	-	Structurally removed	-

2.2 Experimental setup

The experimental investigation was conducted using a laboratory-scale low-head hydropower test rig consisting of a water reservoir, centrifugal circulation pump, discharge control valve, flow measurement system, and turbine testing section, as illustrated in Figure 2. Water discharge was supplied continuously from the reservoir to the turbine inlet under controlled operating conditions. The experimental setup was designed to simulate low-head micro-hydropower applications under steady-state flow conditions.

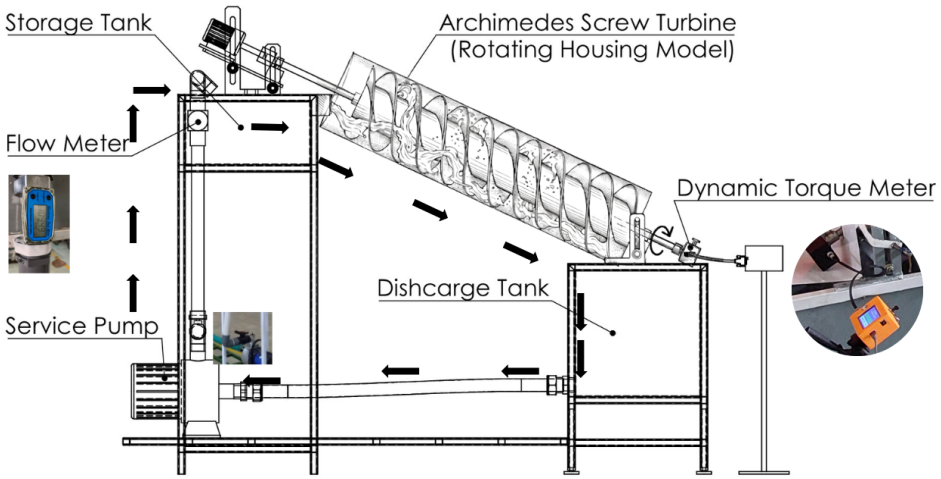

Fig. 2. Schematic diagram of the experimental setup

Torque output and rotational speed were primarily measured using a calibrated dynamic torque meter equipped with an integrated digital tachometer. In addition, a non-contact digital tachometer was employed as an independent verification instrument to validate rotational speed measurements during the experiments. For each experimental run, the inclination angle was first adjusted using a digital inclinometer with an accuracy of ±0.1°, and the discharge was regulated using the flow-control valve. After the hydraulic conditions stabilized, the turbine was allowed to accelerate under the supplied water flow. The braking mechanism of the dynamic torque meter was then progressively adjusted until the rotational speed was maintained at 45 RPM. Therefore, the reported measurements represent controlled-speed, brake-loaded operation rather than free-running conditions. Torque and rotational speed were recorded over a 10–15 s steady-state interval. Each operating condition was independently repeated three times, and the same procedure was applied to both turbine configurations. The experimentally measured flow rate in *L/min* was converted into SI units (*m³/s*) for hydraulic power and efficiency calculations. Similar instrumentation approaches have been widely employed in experimental AST studies to ensure reliable and reproducible measurements [16],[29].

The effective hydraulic head was geometrically determined from the vertical component of the effective installation length, according to $H = L_{eff} \sin\theta$, where $L_{eff} = 1.221$ m represents the effective length of the experimental installation used for head calculation and θ denotes the turbine inclination angle. This effective installation length differs from the turbine axial length of 1.200 m specified in Table 1. The resulting hydraulic heads were 0.4176, 0.5160, and 0.6105 m at inclination angles of 20°, 25°, and 30°, respectively. These head values were used to determine the hydraulic input power and turbine efficiency for the corresponding operating conditions.

The hydraulic power input was calculated using:

$$P_{hyd} = \rho g Q H \tag{1}$$

Where (ρ) is water density (*kg/m³*), (g) is gravitational acceleration (*m/s²*), (Q) is discharge (*m³/s*), and (H) is effective hydraulic head (*m*). The mechanical power output was determined from the measured torque and rotational speed using:

$$P_{mech} = T\omega \tag{2}$$

where (T) is torque (*N·m*) and (ω) is angular velocity (*rad/s*). Hydraulic efficiency was subsequently calculated as:

$$\eta = \frac{P_{mech}}{P_{hyd}} \times 100\% \tag{3}$$

Each experimental condition was repeated three times to ensure data consistency and repeatability. Average values were used for performance evaluation, while deviations between repeated measurements were monitored to assess experimental reliability. The uncertainty of flow rate measurement was within ±2%, while torque and rotational speed measurements exhibited maximum deviations below ±1.5% and ±1%, respectively. The experimental operating conditions investigated in this study are summarized in Table 2.

Table 2. Experimental operating conditions

Parameter	Range
Flow rate (Q)	50–100 L/min
Inclination angle (θ)	20°, 25°, and 30°
Rotational speed	45 RPM
Operating condition	Steady-state

2.3 CFD modeling

Computational Fluid Dynamics (CFD) simulations were conducted to investigate internal flow behavior, pressure distribution, and hydraulic energy transfer mechanisms inside the AST systems. The simulations were performed using ANSYS Fluent 2024 R2. The numerical approach generally followed previous CFD investigations on Archimedes screw turbines [17],[22],[26].

Three-dimensional geometries of the fixed-housing and rotating-housing AST configurations were developed using CAD software and imported into the CFD environment. The computational domain included the screw channels, inlet region, and outlet section to capture internal flow development throughout the turbine. The overall CFD model configuration and computational domain are illustrated in Figure 3. Unstructured tetrahedral meshes with local refinement near blade surfaces and flow interaction regions were employed to improve numerical accuracy. The computational mesh structure used for the rotating-housing AST configuration is presented in Figure 4.

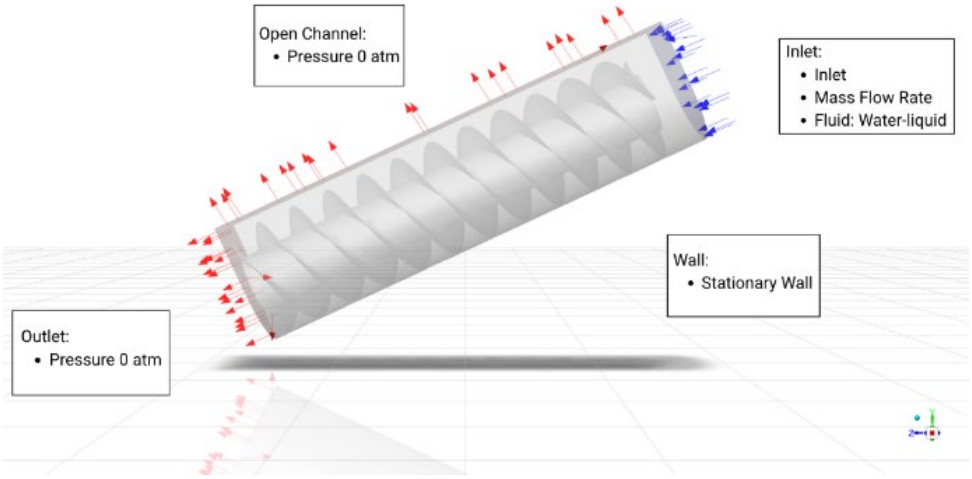

(a)

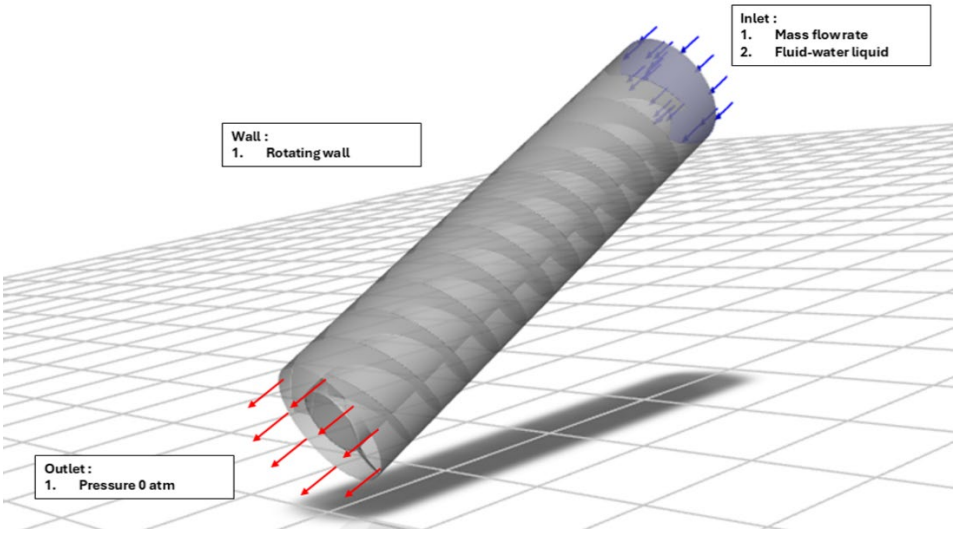

(b)

Fig. 3. CFD model configuration and computational domain; (a) fixed-housing configuration; (b) rotating-housing configuration

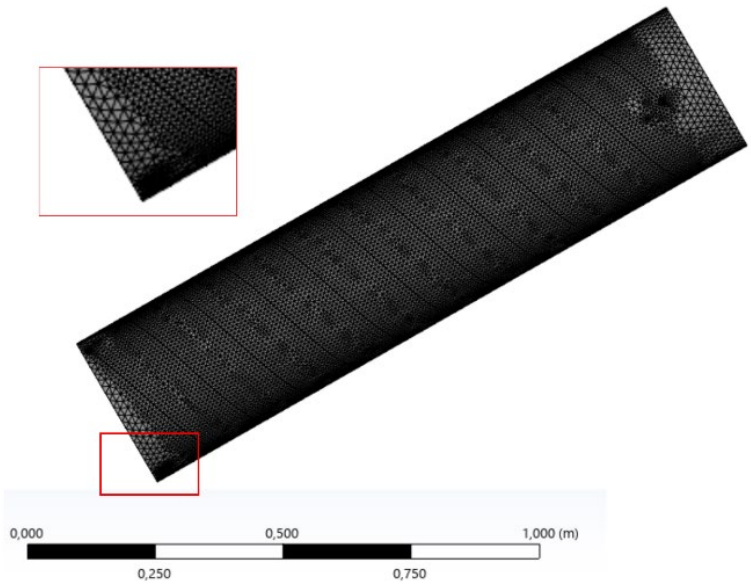

Fig. 4. Computational mesh structure for the rotating-housing AST

A mesh independence study was conducted to assess the sensitivity of the predicted torque to spatial discretization. Four mesh resolutions containing 50,165, 93,160, 202,001, and 604,222 cells were evaluated, producing torque values of 0.574, 0.627, 0.644, and 0.647 Nm, respectively. The relative difference between the two finest meshes was approximately 0.47%, indicating limited sensitivity to further grid refinement for the evaluated operating condition. Consequently, the finest mesh was selected for the subsequent simulations. The final mesh exhibited an average skewness of 0.24 and an average orthogonal quality of 0.75. This assessment establishes grid convergence for the selected condition but does not independently quantify other sources of numerical uncertainty.

The incompressible Reynolds-Averaged Navier–Stokes (RANS) equations were solved using the shear stress transport (SST) k–ω turbulence model to represent wall-bounded flow, adverse pressure gradients, and possible flow separation within the screw channels [31]. The Volume of Fluid (VOF) method was employed to capture the air–water interface and free-surface flow behavior, enabling the representation of multiphase interactions and water occupancy within the turbine [17],[20],[21].

Boundary conditions were defined based on the experimental operating conditions. A mass-flow inlet boundary condition was applied at the turbine inlet, with the inlet mass flow rate calculated from the corresponding experimental volumetric flow rate and water density. A pressure outlet boundary condition was specified at the outlet, with the static pressure set to atmospheric pressure. The rotational motion of the screw assembly was modeled using a rotating reference frame approach at a prescribed rotational speed of 45 RPM, consistent with the experimental operating conditions. Steady-state simulations were performed until residual convergence and stable torque values were achieved.

2.4 Validation strategy

A comparative validation procedure was conducted to evaluate the agreement between CFD predictions and experimental measurements. The validation focused primarily on torque generation because torque directly represents the effectiveness of hydraulic-to-mechanical energy conversion in AST systems.

For each operating condition, the torque values predicted by CFD simulations were compared with experimentally measured torque obtained from the laboratory testing system. The percentage deviation between numerical and experimental results was calculated using:

$$Error(\%) = \frac{\left|T_{exp} - T_{CFD}\right|}{T_{exp}} \times 100 \quad (4)$$

where (T_{exp}) represents the experimentally measured torque and (T_{CFD}) denotes the torque predicted by the CFD simulation.

The validation was performed for both fixed-housing and rotating-housing turbine configurations over the investigated range of flow rates and inclination angles. The resulting deviations were used to evaluate the capability of the numerical model to reproduce the experimentally observed performance trends. The CFD validation results and their implications for flow analysis are presented and discussed in Section 3.

2.5 Predictive modeling

To establish quantitative relationships between operating conditions and turbine performance, predictive modeling was performed using regression-based approaches. The predictive analysis aimed to estimate torque generation,

mechanical power output, and hydraulic efficiency as functions of key operating variables, including flow rate and inclination angle.

Polynomial regression and multivariate regression models were employed to identify nonlinear relationships between operating parameters and performance characteristics. The general multivariate regression form can be expressed as:

$$Y = a + bQ + c\theta + dQ^2 + e\theta^2 + f(Q\theta) \quad (5)$$

where (Y) represents the predicted performance parameter, (Q) is the flow rate, (θ) is the inclination angle, and (a - f) are regression coefficients determined from experimental data fitting. The regression coefficients were obtained using least-squares fitting based on 18 experimental observations collected from the rotating-housing AST configuration.

Response Surface Methodology (RSM) was employed to investigate the combined effects of flow rate and inclination angle on turbine performance and to identify favorable operating conditions within the experimentally investigated domain. The second-order polynomial regression models developed from the experimental dataset were used as empirical response functions for the optimization analysis. Similar regression-based approaches have been applied in previous studies of Archimedes screw turbine performance and parametric optimization [15],[17].

A constrained operating-condition optimization was formulated using the predicted hydraulic efficiency as the primary objective function. The optimization problem was defined as:

$$\max_{Q,\theta} \hat{\eta}(Q,\theta)$$

subject to:

$$50 \leq Q \leq 100 \text{ L/min}$$
$$20^\circ \leq \theta \leq 30^\circ$$

where $\hat{\eta}(Q,\theta)$ represents the hydraulic efficiency predicted by the fitted second-order polynomial model. The constrained maximum was determined by evaluating the response function within the specified parameter bounds, including its stationary conditions and boundary values. The corresponding predicted torque and mechanical power were subsequently calculated using their respective regression equations as supporting performance indicators.

The optimization was restricted to the experimentally investigated ranges of flow rate and inclination angle. Accordingly, the identified solution represents a model-based optimum within the prescribed operating domain rather than a global optimum of the turbine configuration. Because the regression models were fitted using 18 experimental observations, the optimization results were interpreted as preliminary model-assisted operating-condition estimates requiring independent experimental validation.

The predictive capability of the developed models was evaluated using several statistical indicators, including the coefficient of determination (R^2), Root Mean Square Error (RMSE), and Mean Absolute Percentage Error (MAPE). These statistical metrics were used to assess the agreement between predicted and experimental performance values and to quantify the reliability of the developed predictive models. The resulting regression models, statistical validation results, and predictive performance analyses are presented and discussed in Section 3.

3 Results and discussion

3.1 Experimental performance dataset and operating trends

The experimental dataset obtained from the rotating-housing Archimedes screw turbine demonstrates clear relationships between operating conditions and turbine performance. Figure 5 presents the variations of torque, mechanical power, and hydraulic efficiency as functions of flow rate for inclination angles of 20°, 25°, and 30°.

As shown in Figure 5(a), torque increased consistently with increasing flow rate for all investigated inclination angles. The highest torque values were obtained at an inclination angle of 30°, increasing from 0.43 Nm at 50 L/min to 0.99 Nm at 100 L/min. In contrast, the 20° configuration produced the lowest torque throughout the operating range investigated. These results indicate that both flow rate and inclination angle significantly influence the hydrostatic loading acting on the screw blades and consequently affect torque generation.

A similar trend was observed for mechanical power output, as illustrated in Figure 5(b). Since power is directly proportional to torque at a constant rotational speed, mechanical power increased with increasing flow rate for all inclination angles. The maximum power output of 4.65 W was achieved at a flow rate of 100 L/min and an inclination angle of 30°, whereas the lowest value of 0.72 W was recorded at 50 L/min and 20°. The results confirm that higher discharge conditions provide greater hydraulic energy input, enabling more effective energy conversion within the turbine.

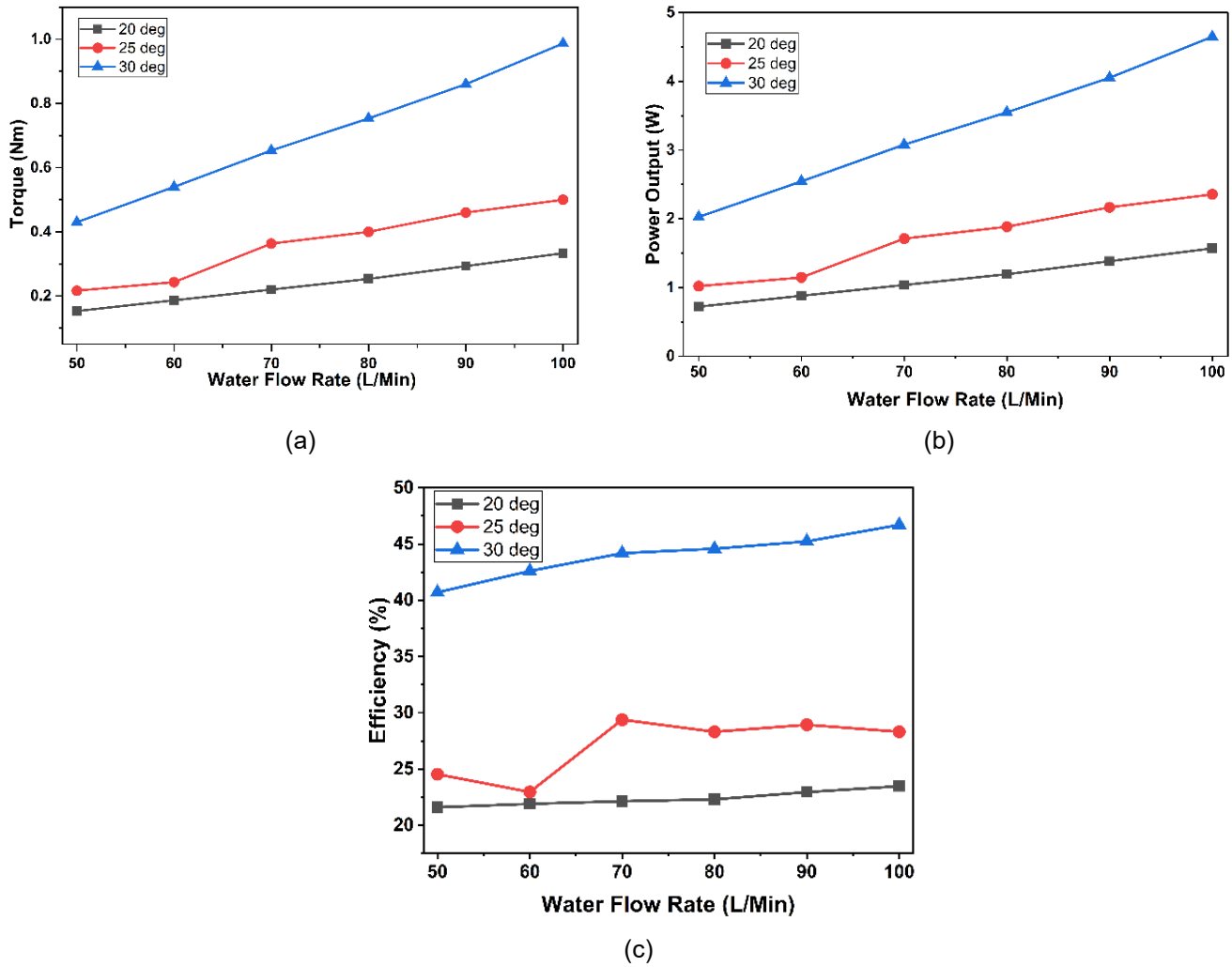

Fig. 5. Experimental performance trends of the rotating-housing Archimedes screw turbine under varying flow rates and inclination angles: (a) torque versus flow rate, (b) mechanical power versus flow rate, and (c) hydraulic efficiency versus flow rate

Figure 5(c) shows the variation of hydraulic efficiency with operating conditions. Although efficiency exhibited a less pronounced increase than torque and power, a general improvement was observed with increasing flow rate and inclination angle. The highest efficiency of 46.71% was obtained at an inclination angle of 30° and a flow rate of 100 L/min. This trend suggests that the rotating-housing configuration maintained favorable water occupancy and hydraulic loading conditions over the investigated operating range, thereby supporting efficient energy conversion.

Table 3. Experimental torque comparison between fixed-housing and rotating-housing AST configurations

Inclination angle (°)	Flow-rate range (L/min)	Mean FH-AST torque (Nm)	Mean RH-AST torque (Nm)	Torque improvement (%)
20	50–100	0.196	0.240	22.73
25	50–100	0.259	0.364	40.56
30	50–100	0.371	0.702	89.07
Note: The reported values represent arithmetic means across six flow-rate conditions at each inclination angle. Torque improvement was calculated from the ratio of the configuration-specific mean torques.				

To further evaluate the performance implications of the rotating-housing configuration, experimental torque measurements were compared with those obtained from the conventional fixed-housing AST under corresponding flow-rate and inclination-angle conditions. As summarized in Table 3, the rotating-housing configuration consistently produced higher mean torque values across the investigated inclination angles. At 20°, the mean torque increased from 0.196 Nm for the fixed-housing configuration to 0.240 Nm for the rotating-housing configuration, corresponding to an improvement of approximately 22.73%. The improvement increased to 40.56% at 25° and 89.07% at 30°, indicating that the performance advantage of the rotating-housing configuration became more pronounced at higher inclination angles.

These results are consistent with the expected hydraulic benefit of structurally removing the conventional blade–housing radial clearance, which provides a potential bypass-flow pathway in fixed-housing turbines. However, because leakage discharge was not directly measured, the observed torque improvements should be interpreted as comparative performance evidence rather than a direct quantification of leakage reduction. The complete paired experimental measurements are provided in the supplementary dataset.

Overall, the experimental dataset exhibits monotonic performance trends and strong parameter sensitivity, providing a reliable basis for CFD validation and subsequent predictive model development. The observed relationships between flow rate, inclination angle, and turbine performance are further explored through numerical simulations and regression-based predictive modeling in the following sections.

3.2 CFD validation and numerical representation of experimental behavior

The numerical model was evaluated by comparing CFD-predicted torque with experimental measurements under identical operating conditions. The comparison covered 36 operating cases, comprising 18 cases for each turbine configuration, with flow rates ranging from 50 to 100 L/min and inclination angles of 20°, 25°, and 30°. As summarized in Table 4, the mean absolute relative deviations were 34.86% for the fixed-housing AST and 23.56% for the rotating-housing AST, with an overall mean deviation of 29.21%. These results indicate that the CFD model captured some general performance trends but exhibited considerable quantitative discrepancies under certain operating conditions.

Table 4. Summary of absolute relative deviations between CFD-predicted and experimentally measured torque

Configuration	Inclination angle (°)	Number of cases	Mean absolute relative deviation (%)	Maximum deviation (%)
Fixed-housing	20	6	19.05	31.54
Fixed-housing	25	6	30.04	55.59
Fixed-housing	30	6	55.48	130.85
Fixed-housing overall	20–30	18	34.86	130.85
Rotating-housing	20	6	13.45	25.85
Rotating-housing	25	6	37.07	51.18
Rotating-housing	30	6	20.17	26.54
Rotating-housing overall	20–30	18	23.56	51.18
All configurations	20–30	36	29.21	130.85
Note: Deviations were calculated relative to experimental torque. Each configuration included 18 operating conditions comprising six flow rates and three inclination angles. The reported mean deviations represent arithmetic averages of absolute relative deviations.				

For the rotating-housing configuration, the deviations ranged from 1.23% to 51.18%, with the largest discrepancy occurring at 100 L/min and 25°. The fixed-housing configuration showed a maximum deviation of 130.85% at 50 L/min and 30°. Such discrepancies may arise from simplifications in representing transient free-surface flow, turbulence, and experimental operating conditions. Previous numerical investigations have highlighted the complexity of multiphase flow and hydraulic interactions in Archimedes screw turbines [17],[21],[22]. However, the individual contributions of these factors to the present deviations were not quantified.

Representative pressure distributions within the rotating-housing AST are illustrated in Fig. 6. Higher-pressure regions are concentrated near the upstream water-filled screw buckets, while pressure generally decreases toward the outlet. This distribution illustrates the hydraulic pressure loading acting on the screw blades and provides a qualitative explanation of torque generation. The interpretation is consistent with previous investigations emphasizing the influence of flow characteristics and hydraulic losses on Archimedes screw turbine performance [21],[22],[25].

Overall, the CFD results provide complementary insight into the hydraulic behavior of the rotating-housing configuration, although their quantitative predictive accuracy remains limited. Therefore, the CFD simulations are used primarily to support the physical interpretation of turbine operation, while the experimental measurements constitute the primary dataset for developing and evaluating the regression-based predictive models presented in Section 3.3.

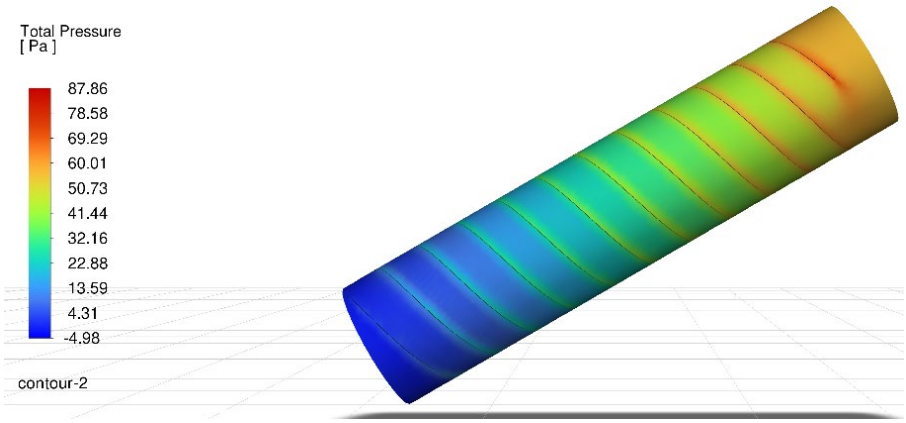

Fig. 6. Representative CFD pressure within the rotating-housing AST

3.3 Development of predictive performance models

Based on the second-order polynomial regression framework described in Section 2.5, predictive models were developed to establish quantitative relationships between flow rate Q, inclination angle θ, and the performance of the rotating-housing Archimedes screw turbine (RH-AST). The regression coefficients were estimated using the ordinary least-squares method based on 18 experimental observations. The verified coefficients for torque, mechanical power, and hydraulic efficiency are presented in Table 5. To ensure numerical reproducibility, sufficient decimal precision was retained in the reported coefficients, particularly for the quadratic and interaction terms.

The resulting predictive equations for torque, mechanical power, and hydraulic efficiency are expressed in Equations (6)-(8), respectively.

Table 5. Regression coefficients of the developed predictive models

Coefficient	Torque Model	Power Model	Efficiency Model
a - intercept	2.783690476	12.998968254	126.870158730
b - Q	−0.011938095	−0.052864286	+0.090776190
c - θ	−0.224857143	−1.059428571	−10.634571429
d - Q^2	≈ 0	−0.000013095238	−0.001273809524
e - θ^2	+0.004300000	+0.020333333	+0.244933333
f - $Q\theta$	+0.000751428571	+0.003485714286	+0.007314285714
Note: Regression coefficients were estimated using 18 experimental observations. The quadratic flow-rate coefficient in the torque model was numerically negligible and is represented as approximately zero.			

Based on these coefficients, the predictive equations for torque, mechanical power, and hydraulic efficiency can be expressed as:

$$T = 2.783690476 - 0.011938095Q - 0.224857143\theta + 0.004300000\theta^2 + 0.000751428571Q\theta \quad (6)$$

$$P = 12.998968254 - 0.052864286Q - 1.059428571\theta - 0.000013095238Q^2 + 0.020333333\theta^2 + 0.003485714286Q\theta \quad (7)$$

$$\eta = 126.870158730 + 0.090776190Q - 10.634571429\theta - 0.001273809524Q^2 + 0.244933333\theta^2 + 0.007314285714Q\theta \quad (8)$$

where (T) is torque (Nm), (P) is mechanical power (W), (η) is hydraulic efficiency (%), (Q) is flow rate (L/min), and (θ) is inclination angle (°). The developed regression models reveal that turbine performance is governed by both the individual effects of flow rate and inclination angle as well as their interaction. The positive interaction coefficients in all three models indicate that the beneficial effect of increasing flow rate becomes more pronounced at larger inclination angles. This finding is consistent with the experimental observations presented in Section 3.1, where the highest performance values were obtained at an inclination angle of 30° and a flow rate of 100 L/min.

The efficiency model exhibited curvature in its fitted response surface, whereas the torque model showed an approximately linear dependence on flow rate at a fixed inclination angle. The relative influence of individual operating parameters should be interpreted within the investigated domain rather than inferred solely from the magnitudes of dimensional regression coefficients.

Figure 7 presents representative response surfaces generated from the developed regression equations. The response surfaces clearly illustrate the combined influence of flow rate and inclination angle on turbine performance

and identify the operating region associated with enhanced torque generation, power production, and hydraulic efficiency. These predictive relationships provide a practical tool for rapid performance estimation and serve as the foundation for the statistical validation and optimization analyses presented in the following sections.

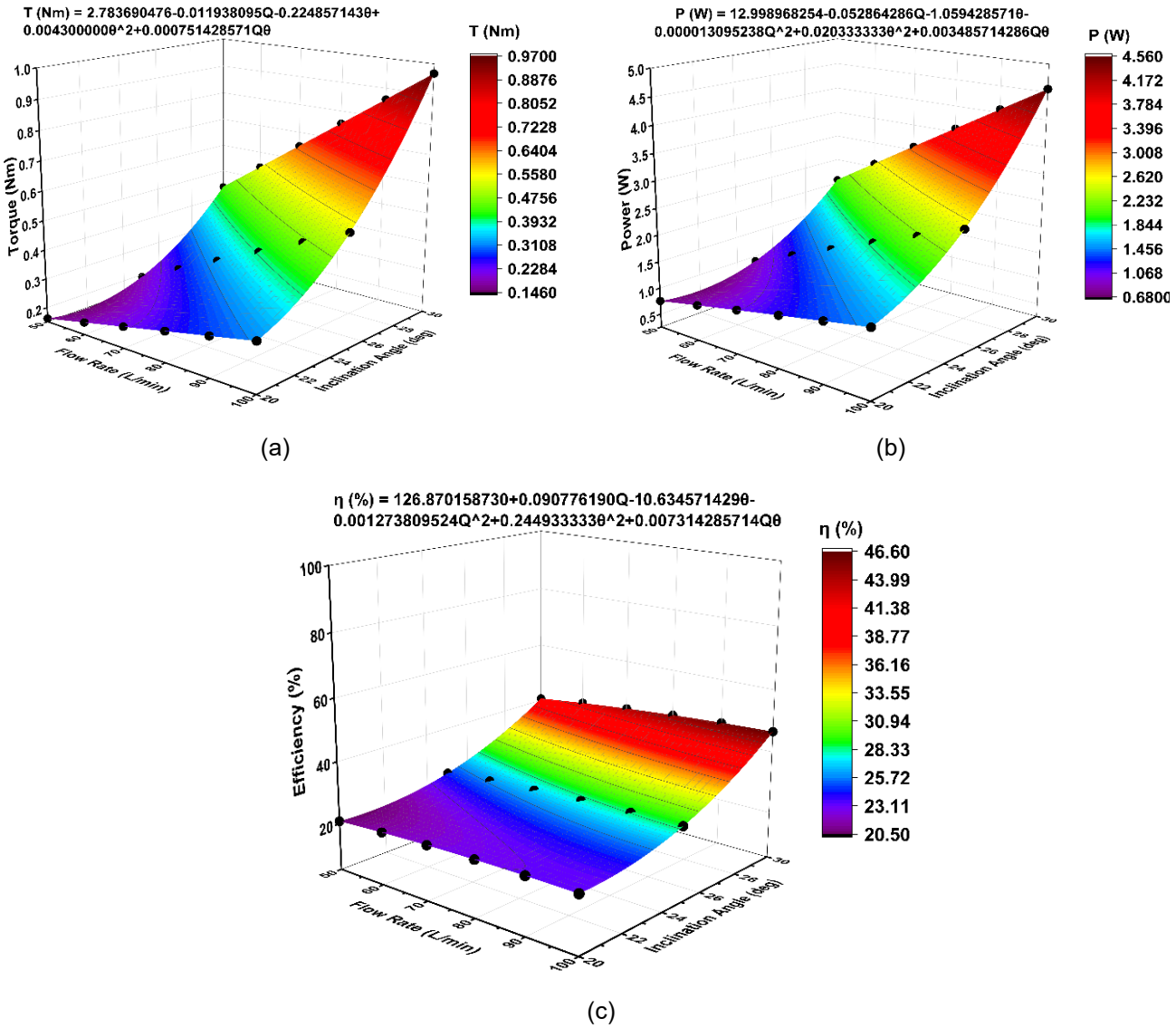

Fig. 7. Response surface representation of the developed predictive models. (a) torque generation, (b) mechanical power output, and (c) hydraulic efficiency

3.4 Statistical evaluation of regression model fit

The goodness of fit of the developed regression models was evaluated using the coefficient of determination (R^2), root mean square error (RMSE) and mean absolute percentage error (MAPE). These metrics were calculated by comparing the fitted values with the experimental observations used to develop the models. The results are summarized in Table 6.

Table 6. Statistical validation parameters of predictive models

Model	R^2	RMSE	MAPE (%)
Torque prediction	0.9956	0.0156	3.4531
Power prediction	0.9959	0.0708	3.3080
Efficiency prediction	0.9892	0.9833	2.3363

The regression models exhibited strong agreement with the experimental dataset, with R^2 values exceeding 0.98 and MAPE values below 5%. The torque and mechanical power models showed particularly high coefficients of determination, while the efficiency model also captured most of the observed variation. The relatively low RMSE values further indicate small fitting errors within the investigated operating domain.

The agreement between measured and fitted responses is illustrated by the regression results and response surfaces presented in Figure 7. However, because the statistical metrics were calculated using the same observations employed for model fitting, they represent in-sample performance rather than independent predictive validation.

Accordingly, the developed equations provide useful empirical estimates of turbine performance within the investigated ranges of 50–100 L/min and 20°–30°. Their predictive capability under new operating conditions requires further assessment using independent experimental measurements.

3.5 Model-based operating-condition optimization and design implications

The developed regression models were employed to identify favorable operating conditions for the rotating-housing Archimedes screw turbine (RH-AST) within the experimentally investigated domain. Figure 8 presents the corresponding performance contour maps, illustrating the combined effects of flow rate and inclination angle on torque, mechanical power, and hydraulic efficiency. The response surfaces generally indicate improved performance at higher flow rates and inclination angles, consistent with the experimental trends discussed in Section 3.1 and previous response-surface optimization studies [15, 19].

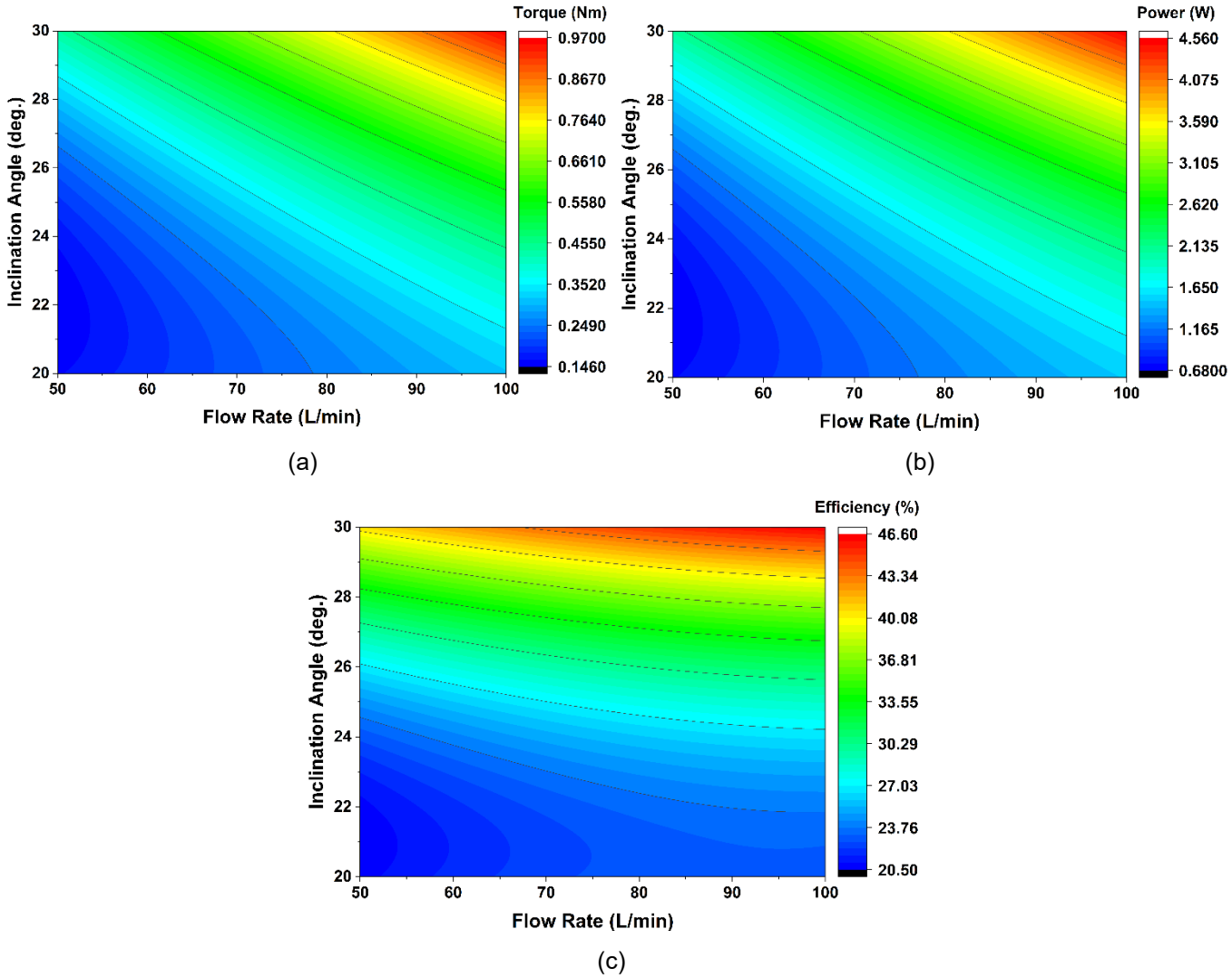

Fig. 8. Model-based performance contour maps of the rotating-housing Archimedes screw turbine showing the combined effects of flow rate and inclination angle on (a) torque, (b) mechanical power, and (c) hydraulic efficiency

The constrained optimization of the hydraulic efficiency model identified a maximum predicted efficiency of 46.56% at a flow rate of 100 L/min and an inclination angle of 30°. At this operating point, the regression models predicted a torque of 0.968 Nm and a mechanical power output of 4.556 W, compared with the experimentally measured values of 0.99 Nm, 4.65 W, and 46.71% for torque, power, and efficiency, respectively. The absolute difference between predicted and measured efficiency was approximately 0.15 percentage points, indicating close agreement at this operating condition.

The identified optimum occurred at the upper boundaries of both operating variables, indicating a domain-constrained rather than a global optimum. Although the fitted response surfaces provide quantitative relationships between operating conditions and turbine performance, their predictive reliability beyond the investigated range remains unverified. Furthermore, because the regression models were developed using the same experimental dataset employed for statistical evaluation, independent experimental validation is required to establish their generalizability.

From an engineering perspective, the developed models provide a computationally efficient tool for preliminary operating-condition assessment of RH-AST systems. The identified operating region may inform the selection of flow rate and inclination angle for low-head micro-hydropower applications, particularly where available hydraulic resources and installation constraints limit operating flexibility [6]. Nevertheless, the results should be interpreted as preliminary design guidance rather than universally applicable operating recommendations.

4 Conclusions

This study evaluated the performance of a leakage-suppressed rotating-housing Archimedes screw turbine (RH-AST) through laboratory experiments, CFD analysis, and regression-based operating-condition optimization. The rotating-housing configuration structurally removed the conventional blade–housing radial clearance, providing an alternative approach to suppressing potential bypass-flow losses. Experimental results demonstrated increasing torque and mechanical power with flow rate and inclination angle, reaching maximum values of 0.99 Nm and 4.65 W, respectively, at 100 L/min and 30°. Comparative measurements further indicated higher torque for the rotating-housing configuration than for the conventional fixed-housing turbine, with the largest mean improvement of 89.07% observed at 30°.

The CFD simulations provided qualitative insight into internal pressure distribution and hydraulic loading but exhibited a mean absolute relative torque deviation of 23.56% for the rotating-housing configuration, indicating limitations in quantitative predictive accuracy. Second-order polynomial regression models showed strong in-sample agreement with experimental observations, achieving R^2 values of 0.9956, 0.9959, and 0.9892 for torque, mechanical power, and hydraulic efficiency, respectively. Constrained optimization identified a maximum predicted efficiency of 46.56% at 100 L/min and 30°, compared with the experimentally measured efficiency of 46.71%. This operating point represents the optimum within the investigated parameter domain rather than a maximum global performance.

Overall, the integration of experimental characterization, CFD analysis, and regression-based optimization provides a preliminary framework for evaluating RH-AST performance and identifying favorable operating conditions in low-head micro-hydropower applications. However, the CFD model requires further refinement, and the regression models require independent validation before their predictive reliability can be established under untested conditions. Future investigations should extend the operating range, examine additional geometric parameters, and evaluate the performance and reliability of rotating-housing turbines under field-scale operating conditions.

5 Acknowledgments

The authors are thankful to the Department of Mechanical Engineering, Universitas Negeri Yogyakarta, for their guidance, technical support, and facilities provided throughout the study.

6 References

[1] Duah, I. K., Sekyere, C. K. K., Kemausuor, F., & Amaning, K. A. (2025). Micro hydropower research and practice over the last decade for advancing decentralized energy access. *Discover Sustainability*. https://doi.org/10.1007/s43621-025-02375-3

[2] Paish, O. (2002). Small hydro power: Technology and current status. *Renewable and Sustainable Energy Reviews, 6,* 537–556. https://doi.org/10.1016/S1364-0321(02)00006-0

[3] Quaranta, E., & Revelli, R. (2018). Gravity water wheels as a micro hydropower energy source: A review based on historic data, design methods, efficiencies and modern optimizations. *Renewable and Sustainable Energy Reviews, 97,* 414–427. https://doi.org/10.1016/j.rser.2018.08.033

[4] Date, A., & Akbarzadeh, A. (2009). Design and cost analysis of low head simple reaction hydro turbine for remote area power supply. *Renewable Energy, 34,* 409–415. https://doi.org/10.1016/j.renene.2008.05.012

[5] Waters, S., & Aggidis, G. A. (2015). Over 2000 years in review: Revival of the Archimedes Screw from pump to turbine. *Renewable and Sustainable Energy Reviews, 51,* 497–505. https://doi.org/10.1016/j.rser.2015.06.028

[6] Rumbayan, M., & Rumbayan, R. (2023). Feasibility study of a micro hydro power plant for rural electrification in Lalumpe Village, North Sulawesi, Indonesia. *Sustainability, 15(19)*, Article 14285. https://doi.org/10.3390/su151914285

[7] Lyons, M., & Lubitz, W. (2013). Archimedes screws for microhydro power generation. In Proceedings of the ASME 2013 7th International Conference on Energy Sustainability and 11th Fuel Cell Science, *Engineering and Technology Conference* (ESFuelCell2013). https://doi.org/10.1115/ES2013-18067

[8] Purece, C., & Corlan, L. (2021). Archimedean screw as fish-friendly turbines for harnessing hydropower potential. *E3S Web of Conferences, 286,* Article 02007. https://doi.org/10.1051/e3sconf/202128602007

[9] Erinofiardi, E., Koirala, R., Shiwakoti, N., & Date, A. (2022). Sustainable power generation using Archimedean screw turbine: Influence of blade number on flow and performance. *Sustainability, 14(23)*, Article 15948. https://doi.org/10.3390/su142315948

[10] Sołowiej, P., & Łapiński, K. (2025). Recent progress in research on the design and use of an Archimedes screw turbine: A review. *Sustainability, 17(1)*, Article 201. https://doi.org/10.3390/su17010201

[11] Shamsuddeen, M. M., Shahzer, M. A., Roh, M. S., & Kim, J. H. (2024). Feasibility study of ultra-low-head hydro turbines for energy extraction from shallow waterways. *Heliyon, 10*, Article e35008. https://doi.org/10.1016/j.heliyon.2024.e35008

[12] Rorres, C. (2000). The turn of the screw: Optimal design of an Archimedes screw. *Journal of Hydraulic Engineering, 126,* 72–80. https://doi.org/10.1061/(ASCE)0733-9429(2000)126:1(72)

[13] Nuernbergk, D., & Rorres, C. (2013). Analytical model for water inflow of an Archimedes screw used in hydropower generation. *Journal of Hydraulic Engineering, 139,* 213–220. https://doi.org/10.1061/(ASCE)HY.1943-7900.0000661

[14] Zamani, M., Shafaghat, R., & Alizadeh, B. (2023). Experimental investigation on the effect of flow rate and load on the hydrodynamic behavior and performance of an Archimedes screw turbine. *International Journal of Engineering, 36*, 733–745. https://doi.org/10.5829/IJE.2023.36.04A.12

[15] Uniyal, V., Karn, A., & Singh, V. P. (2024). Parametric optimization of Archimedes screw turbine by response surface methodology and artificial neural networks. *Renewable Energy and Sustainable Development, 10*, 306–318. https://doi.org/10.21622/RESD.2024.10.2.1008

[16] Dellinger, G., Simmons, S., Lubitz, W. D., Garambois, P. A., & Dellinger, N. (2019). Effect of slope and number of blades on Archimedes screw generator power output. *Renewable Energy, 136,* 896–908. https://doi.org/10.1016/j.renene.2019.01.060

[17] Shahverdi, K., Loni, R., Ghobadian, B., Gohari, S., Marofi, S., & Bellos, E. (2020). Numerical optimization study of Archimedes screw turbine (AST): A case study. *Renewable Energy, 145,* 2130–2143. https://doi.org/10.1016/j.renene.2019.07.124

[18] Simmons, S., Dellinger, G., & Lubitz, W. D. (2023). Effects of parameter scaling on Archimedes screw generator performance. *Energies, 16*, Article 7331. https://doi.org/10.3390/en16217331

[19] Bouvant, M., Betancour, J., Velásquez, L., Rubio-Clemente, A., & Chica, E. (2021). Design optimization of an Archimedes screw turbine for hydrokinetic applications using the response surface methodology. *Renewable Energy, 172*, 941–954. https://doi.org/10.1016/j.renene.2021.03.076

[20] Mohedano-Castillo, M. F., Díaz-Delgado, C., López-Rebollar, B. M., Salinas-Tapia, H., Posadas-Bejarano, A., & Rojas Valdez, D. (2025). Micro-hydropower generation using an Archimedes screw: Parametric performance analysis with CFD. *Fluids, 10,* Article 264. https://doi.org/10.3390/fluids10100264

[21] Shahverdi, K., & Maestre, J. M. (2021). CFD numerical simulation of Archimedes screw turbine with power output analysis. *Ocean Engineering, 231*, Article 108718. https://doi.org/10.1016/j.oceaneng.2021.108718

[22] Edirisinghe, D. S., Yang, H. S., Kim, M. S., Kim, B. H., Gunawardane, S. P., & Lee, Y. H. (2021). Computational flow analysis on a real scale run-of-river Archimedes screw turbine with a high incline angle. *Energies, 14(11)*, Article 3307. https://doi.org/10.3390/en14113307

[23] Lubitz, W. D., Lyons, M., & Simmons, S. (2014). Performance model of Archimedes screw hydro turbines with variable fill level. *Journal of Hydraulic Engineering, 140.* https://doi.org/10.1061/(ASCE)HY.1943-7900.0000922

[24] Simmons, S. C., Dellinger, G., Aliabadi, A., & Lubitz, W. D. (2021). *Dynamic overflow leakage in Archimedes screw generators.* https://doi.org/10.32393/CSME.2021.56

[25] Simmons, S. C., & Lubitz, W. D. (2025). Modelling outlet power loss in Archimedes screw generators. *Flow, 4*. https://doi.org/10.1017/FLO.2024.29

[26] Dellinger, G., Garambois, P. A., Dellinger, N., Dufresne, M., Terfous, A., Vazquez, J., & Ghenaim, A. (2018). Computational fluid dynamics modeling for the design of Archimedes screw generator. *Renewable Energy, 118,* 847–857. https://doi.org/10.1016/j.renene.2017.10.093

[27] Kozyn, A., & Lubitz, W. D. (2017). A power loss model for Archimedes screw generators. *Renewable Energy, 108,* 260–273. https://doi.org/10.1016/j.renene.2017.02.062

[28] Lashofer, A., Hawle, W., Kampel, I., Kaltenberger, F., & Pelikan, B. (2012). State of technology and design guidelines for the Archimedes screw turbine. In Proceedings of Hydro 2012: *Innovative approaches to global challenges.*

[29] Simmons, S. C., & Lubitz, W. (2022). An updated model for gap leakage in Archimedes screw generators. In *Proceedings of the Canadian Society for Mechanical Engineering International Congress 2022 (CSME Congress 2022).* https://doi.org/10.7939/r3-sbrk-8313

[30] Kozyn, A., & Lubitz, W. D. (2015). Experimental validation of gap leakage flow models in Archimedes screw generators. *In Renewable energy in the service of mankind (Vol. 1, pp. 365–375).* https://doi.org/10.1007/978-3-319-17777-9_33

[31] Menter, F. R. (1994). Two-equation eddy-viscosity turbulence models for engineering applications. *AIAA Journal, 32,* 1598–1605. https://doi.org/10.2514/3.12149

7 Conflict of interest statement

The authors declare no conflict of interest.

8 Author contributions

Rahmad Hidayat: Conceptualization, methodology, experimental investigation, CFD simulation, data curation, formal analysis, predictive modeling, visualization, writing – original draft, and writing – review and editing. Heri Wibowo: Supervision, methodology, validation, critical review, and writing – review and editing. Fredy Surahmanto: Supervision, methodology, experimental validation, formal analysis, and writing – review and editing.

9 Data availability statement

The supplementary datasets supporting the findings of this study are provided with the manuscript. Additional experimental records and numerical simulation data are available from the corresponding author upon reasonable request.

10 Supplementary materials

Supplementary data supporting this study are provided in a separate file, including experimental measurements, CFD–experimental comparisons, mesh independence results, and regression modeling datasets. These materials are intended to facilitate verification and reproducibility of the reported findings.

Paper submitted: 20.07.2026.
Paper accepted: 27.10.2026.
This is an open access article distributed under the CC BY 4.0 terms and conditions